



Manufacturing of hemicellulosic oligosaccharides from fast-growing Paulownia wood via autohydrolysis: Microwave versus conventional heating

Pablo G. del Río^{*}, Alba Pérez-Pérez, Gil Garrote, Beatriz Gullón

Universidade de Vigo, Departamento de Enxeñaría Química, Facultade de Ciencias, 32004 Ourense, Spain

ARTICLE INFO

Keywords:

Biorefinery
Autohydrolysis
Microwave
Conventional heating
Oligosaccharides
Enzymatic hydrolysis

ABSTRACT

Microwave hydrothermal treatment (MHT) is considered a sustainable technology for the valorization of lignocellulosic materials, enabling the solubilization of hemicellulosic-derived compounds, especially in the form of oligosaccharides that may present potential in the chemical, pharmaceutical or nutraceutical industries. Hence, MHT at 200 and 230 °C, at severity (S_0) among 2.92–4.66 were performed. $S_0 = 3.98$ permitted the recovery of about 80% of the initial xylan as xylooligosaccharides. In order to compare the effectiveness of MHT, conventional hydrothermal treatment (CHT) was performed at conditions leading to the maximum recovery of oligosaccharides ($S_0 = 3.98$, non-isothermal regime at 203 °C). Despite the structural features of oligomers in the three liquors were very similar, the spent solids presented different enzymatic digestibility, which implied a different effect of the treatments, reaching up to 80% of glucan to glucose conversion for the solid after MHT at 230 °C for 0.5 min. Additionally, CHT consumed 2.1–2.8-fold greater energy than MHT, reflecting that microwave-assisted autohydrolysis is a sustainable and efficient technology to process PW.

1. Introduction

Sustainable development goals (SDGs) entail strategies to enhance the global socio-economic and environmental situation provoked by the great fossil-resource dependence (Solarte-Toro and Cardona-Alzate, 2021). In this framework, biorefineries have a pivotal role to accomplish a greener and more eco-friendly world, by the upgrade of biomass into valuable products and energy vectors (Solarte-Toro et al., 2018), play a part in the bioeconomy establishment and reach the objectives projected in the 2030 agenda (Solarte-Toro and Cardona-Alzate, 2021). Hence, lignocellulosic biomass (LB) is deemed as one of the main alternatives to substitute oil industry-derived products (Li et al., 2021).

Paulownia wood has been underlined as a fast-growing short-rotation hardwood with high potential for the manufacture of high-added value products owing to high biomass production (50 t/(ha yr)) and easy adaptation to adverse environments (del Río et al., 2020a; Domínguez et al., 2020). Since LB is mainly composed of cellulose, hemicelluloses and lignin, its separate valorization via fractionation is encouraged. In this sense, hardwood hemicellulose is an amorphous heteropolymer made up of a backbone of xylose linked with β -(1,4)-glycosidic bonds and partially substituted with other hexoses or

pentoses, besides uronic acids and acetyl groups (Álvarez et al., 2017; Jeong and Lee, 2015). This branched macromolecular structure is easily hydrolyzed to high added-value compounds such as xylooligosaccharides (XO), which may present high potential in the pharmaceutical and food industries due to their health benefits as emerging prebiotics (González-García et al., 2018; Li et al., 2021). In addition, the genus Paulownia is also a rich source of secondary metabolites with antioxidant, anti-inflammatory, and antimicrobial properties. Various preparations made of bark, fruit, xylem, or leaves have been used in traditional Chinese medicine to treat infectious diseases such as hemorrhoid, inflammatory bronchitis, gonorrhoea, asthma, erysipelas, bronchopneumonia, enteritis, high blood pressure, among others (Džugan et al., 2021).

Autohydrolysis is deemed as an ecologically friendly cost-effective treatment for the selective solubilization of hemicelluloses with water as only reagent that can be used as first step of a biorefinery (Dávila et al., 2021; Domínguez et al., 2020). Although conventional autohydrolysis is usually based on convection-conduction heating, this strategy is not completely efficient since there is a loss of energy in the transmission of heat through the vessel. However, autohydrolysis assisted by microwave radiation is considered a faster and more efficient

^{*} Corresponding author.

E-mail address: pdelrio@uvigo.es (P.G. del Río).

<https://doi.org/10.1016/j.indcrop.2022.115313>

Received 8 March 2022; Received in revised form 28 June 2022; Accepted 2 July 2022

Available online 12 July 2022

0926-6690/© 2022 The Authors. Published by Elsevier B.V. This is an open access article under the CC BY-NC-ND license (<http://creativecommons.org/licenses/by-nc-nd/4.0/>).

technology due to the direct conversion of electromagnetic energy into heat, and the uniform transmission of heat to the biomass and the solvent (Dávila et al., 2021; del Río et al., 2021; López-Linares et al., 2019).

Despite the increasing number of publications regarding the use of microwave for biomass fractionation, the literature regarding the different effect of heating over the LB is scant. For instance, Aguilar-Reynosa et al. (2017) compared the effect of conventional and microwave heating in the saccharides composition obtained from corn residues, and the suitability of the resulting solid for bioethanol production. Moreover, Dávila et al. (2021) employed vine shoots to study the influence of heating in the production of hemicellulosic oligosaccharides. In this sense, not only the hemicellulosic solubilization can be affected by the type of heating, but also the breakdown of the biomass structure, that can be studied via microscopy techniques and enzymatic susceptibility assays, basic for the obtaining of biofuels such as bioethanol.

In this sense, the chief aim of this study relies on the influence of different heating strategies (conventional and microwaves) in the solubilization of hemicelluloses. Liquors from the optimal conditions for the obtainment of oligosaccharides were subjected to structural analysis (measured via FTIR, MALDI-TOF-MS and HPAEC-PAD), antioxidant capacity of the present phenolics (TPC, TFC, ABTS, DPPH and FRAP) and tentative identification of compounds in the ethyl acetate extract of the liquors. Besides that, the resulting solid phase was chemically characterized and subjected to SEM and enzymatic saccharification, and the energy consumption was evaluated.

2. Materials and methods

2.1. Raw materials and chemical characterization

Paulownia elongata x fortunei wood was used as biomass in the current study, being provided by a local business (Maderas Álvarez Oroza S. L., NW Spain). Firstly, the bark was removed and Paulownia wood (PW) was milled to a particle size ≤ 1 mm after air-dried. The homogeneous lot was conserved in a cool, dark and dry environment.

After the biomass preparation (debarking and milling), PW was chemically characterized using NREL analytical procedures for content in moisture (Sluiter et al., 2008a), ash (Sluiter et al., 2008b), extractives (Sluiter et al., 2008d) and quantitative acid hydrolysis (Sluiter et al., 2008c). Protein content was determined by Kjeldahl method, and the obtained data of nitrogen content was converted via rectification factor for lignocellulosic materials (6.25) (Sluiter et al., 2010). All evaluations were assessed in three replicates.

The solid residue acquired after quantitative acid hydrolysis of the extracts-free biomasses was weighted and identified as Klason lignin. The liquid fraction of quantitative acid hydrolysis was subjected to high performance liquid chromatography (HPLC) analysis to evaluate the amount of monosaccharides and organic acids for the determination of polysaccharides and organic groups. The conditions employed in the HPLC (Agilent, CA, USA) were: Rezex ROA-Organic Acid H+ (8%) column (Phenomenex, CA, USA) at a temperature of 60 °C, flow rate of 0.6 mL/min using as mobile phase 3 mM H₂SO₄ and a refractive index detector at a temperature of 40 °C. In addition, the uronic acids (quantified as equivalents in galacturonic acid) were determined via colorimetric procedure of the liquid after quantitative acid hydrolysis (Blumenkrantz and Asboe-Hansen, 1973).

After thorough characterization, the chemical composition of PW, quantified as g of component/100 g raw material on dry basis \pm standard deviation, was as hereunder (del Río et al., 2020a): glucan 42.2 \pm 0.13, xylan 17.3 \pm 0.03, arabinan 0.84 \pm 0.01, acetyl groups 3.76 \pm 0.03, Klason lignin 20.7 \pm 0.15, extractives 5.21 \pm 0.00, ashes 0.53 \pm 0.00, uronic acids 6.56 \pm 0.10.

2.2. Microwave hydrothermal treatment (MHT)

PW and water were blended at a consistency (C) of 6 g of dry biomass/100 g of total weight in a standard 30 mL Pyrex vessel (G30) and used in microwave hydrothermal treatment (MHT). The equipment consisted in a Monowave 450 single-mode microwave reactor (Anton Paar GmbH, Austria) combined with an air compressor as cooling system. The heating time selected was 5 min for Paulownia as performed in a previous study by the authors (del Río et al., 2021), whereas the cooling time depended on the air compressor and accounted for 5–6 min. The temperature was quantified via infrared detector and the agitation was maintained at 900 rpm via magnetic stirring.

In order to achieve a better comparison among different results and bibliography, the harshness of the treatment, expressed in terms of severity (S_0) and based on the variation of temperature with time (bearing in mind the periods of heating, treatment and cooling) was calculated (del Río et al., 2021):

$$S_0 = \log R_0 = \log(R_{0\text{HEATING}} + R_{0\text{ISOTHERMAL}} + R_{0\text{COOLING}}) = \quad (1)$$

$$= \log \left(\int_0^{t_H} \exp\left(-\frac{T(t) - T_{\text{REF}}}{\omega}\right) \cdot dt + \exp\left(-\frac{T_{\text{ISOT}} - T_{\text{REF}}}{\omega}\right) \cdot t_{\text{ISOT}} + \int_{t_H+t_{\text{ISOT}}}^{t_H+t_{\text{ISOT}}+t_C} \exp\left(-\frac{T'(t) - T_{\text{REF}}}{\omega}\right) \cdot dt \right)$$

where R_0 is the severity factor, $T(t)$ and $T'(t)$ denotes the temperature profiles in the heating and cooling periods respectively, t_H (min) denotes the time needed to achieve the target temperature T_{ISOT} (°C), the temperature that is used in the isothermal processing for a time t_{ISOT} (min), t_C (min) is the time used in the cooling stage, ω describes the empiric parameter related to activation energy and T_{REF} describes the temperature of reference (typical values: $\omega = 14.75$ °C and $T_{\text{REF}} = 100$ °C).

PW was processed at temperatures of 200 °C (0–50 min) and 230 °C (0–6 min), corresponding to severities (S_0) between 2.92 and 4.66. The power employed by the microwave reactor was automatically selected by the equipment to fulfill the set conditions of heating and residence time. However, the power employed never exceeded 400 W, and the energy consumed in the process of heating was measured by the microwave equipment itself and used for the calculation of the energy consumption.

2.3. Conventional hydrothermal treatment (CHT)

PW and water were mixed at a C of 6 g of dry biomass/100 g of total weight in a high-pressure reactor (Büchiglasuster versoclave, Switzerland) of 1.6 L, equipped with temperature control, external fabric mantel as heater and internal water flow for cooling purposes. It was stirred at approximately 500 rpm and heated to a severity of 3.98 (which corresponded to 203 °C in non-isothermal regime) which conduced to maximum recovery of xylooligosaccharides as stated by a previous study by the authors (del Río et al., 2020a). The energy consumed by the equipment was measured by a power-meter (Zaeel) and used for the calculation of the energy consumption.

2.4. Chemical analysis after hydrothermal processing

Once the biomasses were subjected to MHT and CHT, the resulting slurry was filtered to separate the liquid (liquor) and solid fractions. The liquor was stored at 4 °C and used for (i) non-volatile content (oven in 105 °C for 24 h), (ii) direct analysis via HPLC, and (iii) acid post-hydrolysis (4% w/w H₂SO₄, 121 °C and 20 min) analysis via HPLC. The solid fraction was washed using distilled water until neutrality, subjected to gravimetric quantification to assess the solubilization percentage and assayed by quantitative acid hydrolysis as described in a previous section. Experiments were performed in three replicates.

2.5. Determination of phenolic content (TPC) and total flavonoids content (TFC)

Folin Ciocalteu's method (Singleton and Rossi, 1965) with slight variations was employed as technique for the evaluation of TPC of the liquors obtained after hydrothermal treatment. Concisely, the liquor was diluted as desired and a 500 μL aliquot was blended with 2500 μL of Folin Ciocalteu reagent diluted in water at a ratio of 1:10 (v/v). The blend was meticulously stirred in a vortex before adding 2000 μL of Na_2CO_3 (concentration of 75 mg/mL). The trials were incubated at room temperature during 1 h prior to absorbance measure at 760 nm. Gallic acid was used as standard and the results were defined as mg gallic acid equivalent (GAE)/g raw PW. TPC assays were performed in triplicate.

The colorimetric method of aluminum chloride was employed for flavonoids quantification, as explained by (Blasa et al., 2005). Rutin was employed as standard and the results were defined as mg of rutin equivalent (RE)/g raw PW. TFC assays were carried out in triplicate.

2.6. Antioxidant capacity

The antioxidant capacity was performed by the hereunder evaluations: α, α -Diphenyl- β -picrylhydrazyl radical scavenging assay (DPPH), the 2,2-azino-bis-3-ethylbenzothiazoline-6-sulfonic acid radical cation decolorization assay (ABTS) and the ferric reducing antioxidant power (FRAP) employing the procedures described by Gullón et al. (2017a, 2017b). Trolox was used as standard, and the results were defined as mg of Trolox equivalents (TE)/g raw PW. Antioxidant capacity assays were carried out in triplicate.

2.7. Fourier-transformed infrared spectroscopy (FTIR)

The raw material, the spent solids, and the freeze-dried liquors obtained during MHT and CHT were subjected to FTIR analysis in a Nicolet 6700 equipment by Thermo-Scientific (USA). The pellet was prepared with KBr and measured with IR source and DTGS KBr detector. The spectral range studied was from 400 to 4000 cm^{-1} with a resolution of 4 cm^{-1} and 32 scans per min.

2.8. High performance anion exchange chromatography with pulsed amperometric detection (HPAEC-PAD)

HPAEC-PAD was employed in order to identify the degree of polymerization (DP) of oligosaccharides employing the protocol used by Gullón et al. (2014). The equipment used was an ICS3000 chromatographic system (Dionex, Sunnyvale, CA, USA) combined with a Carbo-Pac PA-1 column. Xylooligosaccharides (DP2-DP6) from Megazyme were employed as calibration standards.

2.9. Matrix-assisted laser desorption/ionization-time of flight-mass spectrometry (MALDI-TOF-MS)

Freeze-dried liquors were subjected to MALDI-TOF-MS analysis via an autoflex TOF/TOF equipment (Bruker, MA, USA) employing the protocol used by (Gullón et al., 2014). The samples were diluted (1 mg/mL) in 0.1% trifluoroacetic acid and were applied to the MALDI plate 1:1 with a matrix of 50% 2,5-dihydroxy-benzoic acid 0.1% acetonitrile/trifluoroacetic acid. Analysis were performed in positive refractor mode at a mass range of 500–3500 m/z , using a nitrogen laser ($\lambda = 337 \text{ nm}$).

2.10. Identification of major phenolic compounds using HPLC-ESI-MS

PW liquors were subjected to liquid-liquid extraction employing ethyl acetate using a liquor:solvent ratio of 1:1 (v/v) at room temperature for 30 min with continuous agitation. Both organic and aqueous fractions were isolated by decantation and the extraction of the aqueous

phase was repeated up to 3 times. The resulting organic phase containing the ethyl acetate soluble compounds was vacuum-evaporated at 40 °C and re-dissolved in methanol for further phenolic compounds identification. For that, high performance liquid chromatography fitted with ion mobility spectrometry and time of flight high resolution mass spectrometry (HPLC-ESI-MS) was employed. Samples were introduced into a ZORBAX Eclipse XDB-C18 rapid resolution HD (2.1 \times 100mm 1.8 μm of Agilent) and liquid chromatography separation was performed with an Elute UHPLC (Bruker Daltonics), using the following mobile phases at 0.4 mL/min: 0.1% formic acid (solvent A) and 0.1% formic acid in acetonitrile (solvent B). The gradients consisted on: 2% solvent B for 2 min, 2–30% solvent B for 13 min, 30–100% solvent B for 2 min, 100% solvent B for 4 min, 100–2% solvent B for 1 min, and 2% solvent B for 2 min. The ionization of the samples was produced with an ESI source in negative ion mode using the commonly used operational conditions of 3000 V capillary voltage, 500 V end plate offset, 2 bar nebulizer pressure, 8.0 L/min dry gas, 220 °C dry heater. Accurate mass data, isotopic pattern matching (mSigma value), retention time (using the available standards) and the compounds reported in the bibliography were used for identifying the metabolites.

2.11. Scanning electronic microscopy (SEM)

Micrographs of raw PW, and PW after the autohydrolysis process (MHT at 200 °C for 10 min, MHT at 230 °C for 0.5 min, and CHT at 203 °C) were obtained via a FEI Quanta 200 FEG scanning electronic microscopy (OR, USA) employing 5.0 kV of voltage.

2.12. Enzymatic susceptibility of the solids after hydrothermal processing

Pretreated PW was employed for saccharification to test their enzymatic digestibility. Assays were placed in an orbital incubator equipped with temperature control at conditions of; consistency (C) 5 g of biomass on dry basis/100 g of total weight, 50 °C, 150 rpm, pH= 5 (adjusted with 0.05 N citrate buffer) and cellulase to substrate ratio (CSR) 20 FPU/g. At set times, the assays were sampled and the aliquot was centrifuged at 15,000 rpm for 10 min. Subsequently, the supernatant was filtrated via 0.45 μm nylon membranes and analyzed via HPLC for glucose determination.

The enzymatic cocktail Cellic CTec2 was employed, kindly provided by Novozymes (Denmark). The cellulase activity of Cellic CTec2 was quantified following NREL protocol (Adney and Baker, 2008) with a final activity of 116 FPU/mL.

The resulting glucose production was measured as concentration (g/L) and as glucan to glucose conversion (GGC, %), which is determined as hereunder:

$$GGC = \frac{G_t - G_{t=0}}{\frac{G_n}{100} \cdot \frac{180}{162} \cdot \frac{\rho}{C} - \frac{KL}{100}} \cdot 100\% \quad (2)$$

where G_t denotes the amount of glucose (g/L) at a time t and $G_{t=0}$ denotes the glucose amount (g/L) at the beginning of the assay. G_n denotes the glucan content per 100 g of pretreated PW, 180/162 is the stoichiometric factor for glucan hydration concerning hydrolysis, ρ describes the density of the medium (commonly using 1005 g/L), C denotes the consistency in the experiment, represented in g of solid per 100 g of total weight, and KL represents the g of Klason lignin per 100 g of pretreated biomass.

Results from enzymatic hydrolysis assays can be fitted to empirical model defined by (Holtzaple et al., 1984):

$$GGC_t = GGC_{MAX} \cdot \frac{t}{t + t_{1/2}} \quad (3)$$

where GGC_{MAX} and $t_{1/2}$ are fitting parameters accounting the maximum glucose conversion (%) reachable at infinite reaction time, and $t_{1/2}$ (h) quantifies the reaction time necessary to achieve a glucose conversion of

50% of GGC_{MAX} .

2.13. Statistical analysis

Data resulting from TPC, TFC, DPPH, ABTS and FRAP (measured as mean values \pm standard deviation), were statistically analyzed utilizing the software R (version 4.1.0). Differences among each assay were tested with a one-way ANOVA (analysis of variance) in addition to a Tukey's test. Differences were considered as statistically significant when $p < 0.05$.

3. Results and discussion

3.1. Chemical composition of the liquors obtained during the microwave hydrothermal treatment and conventional hydrothermal treatment

In the current work, microwave hydrothermal treatment (MHT) was applied as green and sustainable strategy for the selective fractionation of Paulownia wood. The reaction mechanism involved in the hydrothermal processing, including the solubilization of hemicellulosic fraction in the form of oligomers, the formation of monomers by breaking of the oligomers and the degradation of monomers into decomposition products, has been extensively studied for different raw materials (del Río et al., 2021; Gullón et al., 2018a; Rico et al., 2018). In this sense, the liquors obtained by microwave-assisted autohydrolysis of Paulownia contained oligosaccharides and monosaccharides, sugar degradation products and phenolic compounds. Fig. 1 depicts the concentration profiles of carbohydrates and degradation compounds in the liquor obtained by microwave-assisted treatment at 200 and 230 °C as a function of the reaction time. As it can be seen in Fig. 1a and d, the oligosaccharide amount increased with the reaction time until a maximum was reached, and then it commenced to decrease. Xylooligosaccharides (XO) were the dominant carbohydrate present in the reaction media for the two temperatures evaluated, with a maximum concentration of 9.40–9.48 g/L, which corresponded to around 80% of conversion of the initial xylan. However, the time required to reach this maximum was different depending on the tested temperature: 0.5 min were needed for the treatment at 230 °C while in the one carried out at 200 °C, 10 min were required (which corresponded to a severity of 3.98 for both

experiments). At harsher conditions, the XO concentration decreased until 1.99 g/L at 200 °C for 50 min and 2.45 g/L at 230 °C for 6 min. Similar operating conditions for optimal xylan solubilization into XO were also reported by other authors from various feedstock. For instance, conduction–convection heating autohydrolysis of peanut shells resulted in a concentration of XO of 9.80 g/L operating at $S_0 = 4.09$ (Rico et al., 2018) and from vine shoots of 12.2 g/L at $S_0 = 4.01$ (Dávila et al., 2016). However, in another study dealing with the microwave hydrothermal treatment of corn stover, it was found that the maximum concentrations of soluble xylan-derived compounds (13.4 g/L) took place under milder operational conditions ($S_0 = 3.43$) than those obtained here (Aguilar-Reynosa et al., 2017).

In addition to XO, acetyl groups linked to oligomers (AcO), glucooligosaccharides (GO) and arabinooligosaccharides (ArO) were identified in lesser concentrations in the autohydrolysis liquors. Regarding the concentration profile of AcO depicted in Fig. 1a and d, it can be noted that the behavior was equivalent to XO, attaining a maximum of 2.22 g/L at the severity of 3.90, while the most severe conditions caused a reduction in concentration until 0.70 g/L at 230 °C and 6 min and its complete depletion in the experiment carried out at 200 °C and 50 min. The GO concentration was low and under the conditions conducting to a higher production of XO ($S_0 = 3.98$) 0.98 g/L (180 °C for 10 min) and 0.69 g/L (230 °C for 0.5 min) were obtained. Similar GO concentrations were also reported by (Aguilar-Reynosa et al., 2017) using corn stover as raw material, obtaining 0.89 g/L at $S_0 = 3.43$ and 1.73 g/L at $S_0 = 3.86$ (corresponding to high XO yielding conditions) using microwave heating processing and conduction-convection heating, respectively. The arabinosyl groups linked to oligomers (ArO) concentration increased to 0.54 g/L (corresponding to a conversion of 94% of arabinan in raw material) operating at $S_0 = 4.15$, then decreased until 0.13 g/L at the harsher conditions ($S_0 = 4.65$).

As expected, high severities promoted hydrolysis and decomposition reactions, which led to a lessening in the formation of oligomers (up to 3.94 times lower at $S_0 = 4.65$) and a growth in the monosaccharides and degradation compounds content. As it can be seen in Fig. 1b and e, the concentration of total monosaccharides (glucose, xylose and arabinose) in the liquors augmented progressively with the elongation of the residence time, from 1.35 to 3.34 g/L at S_0 of 2.92 and 4.65, respectively. Xylose represented the most abundant monosaccharide, achieving the

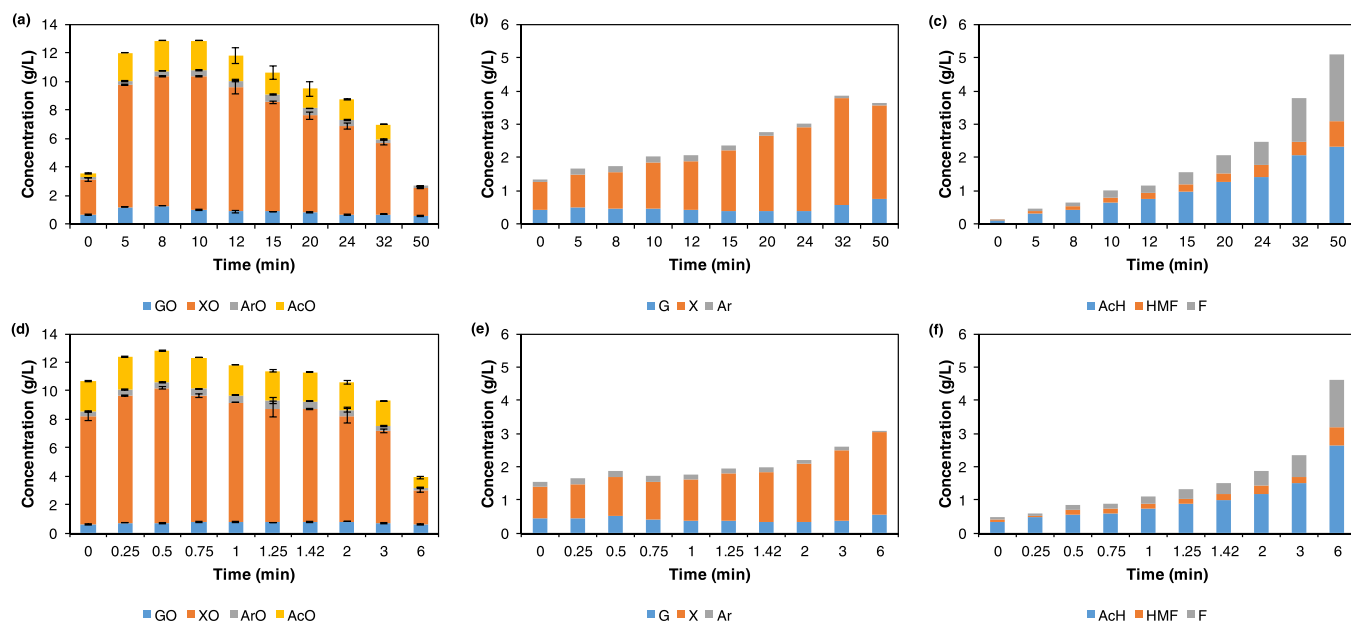


Fig. 1. Chemical composition of the liquors after MHT at (a, b, c) 200 and (d, e, f) 230 °C for oligomers (GO, glucooligosaccharides; XO, xylooligosaccharides; ArO, arabinooligosaccharides; AcO, acetyl groups linked to oligosaccharides), monomers (G, glucose; X, xylose; Ar, arabinose) and organic acids and furans (AcH, acetic acid; HMF, hydroxymethylfurfural; F, furfural).

maximum concentration (3.23 g/L) at 200 °C for 32 min ($S_0 = 4.46$). Glucose was identified at lower concentrations, achieving a maximum value at the severest condition evaluated (0.80 g/L). The concentration of arabinose barely ranged at low and intermediate severities (2.92–3.98) with a value between 0.10 and 0.20 g/L, while at higher severities decreased to concentrations close to zero.

Other compounds observed in the liquors include acetic acid, hydroxymethylfurfural and furfural, which are generated as a result of the hydrolysis of the acetyl groups and dehydration of the monosaccharides (Gullón et al., 2018a; Jönsson and Martín, 2016) and are displayed in Fig. 1c and f. The concentration of these compounds raised steadily with the severity of treatment, and under the severest conditions assayed, acetic acid reached 2.47 g/L, HMF 0.66 g/L and furfural 1.73 g/L. These results are in agreement with those found by (Aguilar-Reynosa et al., 2017) for the autohydrolysis of corn stover (4.88 g/L of total degradation products) under similar operational conditions to the ones used here ($S_0 = 4.66$) and were comparatively lower than that obtained for vine shoots (7.72 g/L of total degradation products) operating at $S_0 = 4.65$ (Dávila et al., 2016).

It is important to underline that in the experiment leading to higher total oligosaccharides production (12.9 g/L at $S_0 = 3.98$) the overall concentration of monomeric sugars was 1.95 g/L; while the joint contribution of organic acids and furans achieved 0.92 g/L. Under the conditions evaluated, the oligosaccharides to monosaccharide mass ratio was of 6.6, which is in line with the values reported by (Rico et al., 2018) for peanut shells (about 5) and is considerably lower than those obtained by (Dávila et al., 2016) for vine shoot (about 20).

In order to compare the effect of the heating mechanism, the MHT conditions that permitted maximizing the production of XO ($S_0 = 3.98$) were simulated using conduction–convection heating (known as conventional autohydrolysis). For this, an experiment was carried out under non-isothermal conditions at $S_0 = 203$ °C (which corresponds to the same MHT treatment severity) in a Büchiglasuster reactor.

When comparing both heating systems on the composition of the liquors, some differences were observed. Regarding the concentration of total oligosaccharides, the treatment by autohydrolysis via conventional hydrothermal treatment (CHT) enabled to obtain a hydrolysate with a concentration of 11.8 g/L, which is 8.4% less than that obtained by microwave-assisted autohydrolysis (see Table 1). On the other hand, the concentration of monomeric sugars concentration was higher in the treatment performed by CHT (2.61 g/L vs 1.95 g/L). In the case of decomposition compounds, slightly higher concentrations were also determined when carrying out the conduction-convection hydrothermal treatment. In this case, the joint contribution of acetic acid, HMF and furfural reached 1.22 g/L, in comparison to 0.92 g/L with MHT. This can be attributed to the fact that in the treatment carried out by CHT, the liquor remains longer at high temperatures, which favors the hydrolysis of the oligosaccharides into monomeric sugars and its subsequent dehydration to degradation compounds.

Table 1

Chemical characterization of PW after non-isothermal conventional hydrothermal treatment (CHT) at 203 °C, corresponding to $S_0 = 3.98$.

Solubilization (g/100 f g raw PW)	30.7
Solid fraction (g/100 g pretreated PW)	
Glucan	58.2 ± 0.64
Hemicelluloses	5.85 ± 0.14
Lignin	29.8 ± 1.03
Liquid fraction (g/L)	
Oligomers	11.8
Monomers	2.61
Acetic acid, HMF and furfural	1.22

3.2. Structural characterization of the oligosaccharides presents in the autohydrolysis liquors

In order to obtain a more detailed interpretation of the structure of oligosaccharides, the liquid fraction acquired after CHT at 203 °C and MHT performed at 200 °C for 10 min and at 230 °C for 0.5 min were analyzed by HPAEC-PAD, MALDI-TOF-MS, and FTIR. As far as the authors know, this is the first time that the oligosaccharides' structure from Paulownia wood obtained by hydrothermal processing is described in detail.

The HPAEC-PAD elution profile of the three liquors is display in the Fig. 2. The chromatograms corroborated the predominance of oligosaccharides with low- or medium-DP, not observing differences in the profile of compounds between the three treatments evaluated. Regarding the substitution pattern, HPAEC-PAD does not allow to determine the presence of acetylated oligomers, because the mobile phase used (highly alkaline solution) during elution causes the saponification of the sample (Dávila et al., 2019; Rivas et al., 2020).

The DP of the XO was also determined using MALDI-TOF-MS. In the spectra of the three liquors, signals with the same m/z but showing dissimilar intensities were observed, which may suggest differences in the quantity of each compound present in the liquid fractions. The tentative assignment of the structure of the compounds present in the liquors is displayed in Table S1 and it was performed considering that the oligosaccharides may be identified as potassium or sodium adducts (Gullón et al., 2018a; Rico et al., 2018). The main identified oligosaccharide series were constituted of pentose chains with a DP ranging from 3 to 14 (made up of xylose units regarding the composition data) highly substituted by acetyl and methylglucuronosyl groups. Moreover, this methodology also revealed that the XO may be partially substituted with hexoses (principally glucose).

The structural features of the oligosaccharides acquired from PW are similar to those published for other oligomers produced by hydrothermal processing of different feedstocks. For instance, Rivas et al. (2020) confirmed the existence of pentaoligomers with a DP in the range of 3–13 and a complex substitution pattern by acetyl groups and O-methyl-uronic units in purified autohydrolysis liquors from poplar; and Dávila et al. (2019) also identified hemicellulosic saccharides composed by a backbone of pentose ranging from 3 to 18 and with substituents such as hexoses, acetyl and methylglucuronosyl groups in refined hydrolysates obtained from vine shoots. These results suggested that the structure of the oligosaccharides obtained under different treatment conditions were similar to each other.

FTIR spectroscopy was employed to detect specific molecular structures in the liquors of the different hydrothermal treatments from PW.

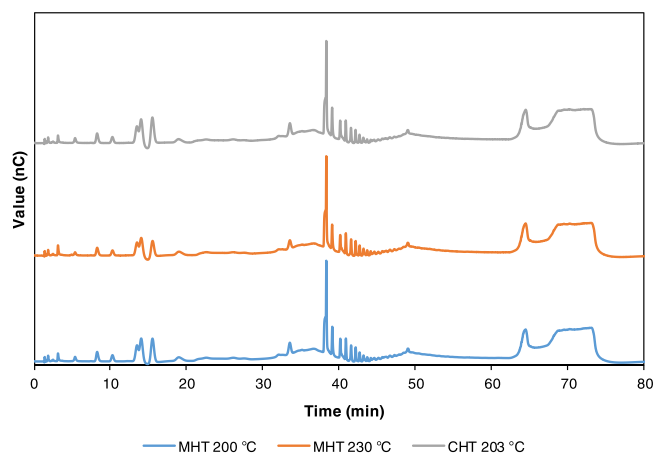


Fig. 2. HPAEC-PAD chromatogram the liquors after microwave hydrothermal treatment at 200 °C for 10 min, and 230 °C for 0.5 min, and conventional hydrothermal treatment at 203 °C.

As can be seen from Fig. 3a, all the absorbance bands occurred simultaneously in the spectra recorded of the liquors obtained in the conventionally heated autohydrolysis treatment and in the microwave-assisted autohydrolysis process, indicating that the main structures of the hemicellulosic oligosaccharides in the three samples were similar to each other. The FTIR spectra of the three samples presented a typical signal pattern of hemicellulose-derived compounds (Dávila et al., 2021, 2016; Gullón et al., 2018a; Jiang et al., 2014; Rico et al., 2018). The signal at 1035 cm^{-1} was ascribed to the stretching and bending vibrations of C-O, C-C, C-OH and the glycosidic C-O-C, confirming the predominance of xylooligosaccharides, what it was in agreement with the results obtained in the composition analysis of the liquors (Dávila et al., 2021). According to the literature the small band located at 895 cm^{-1} could correspond to the β -(1-4)-glycosidic bonds between xylose units in the main xylan chain (Dávila et al., 2016; Gullón et al., 2018a).

The presence of arabinosyl groups in the XO backbone was revealed in the bands at 1146 , 1070 and 988 cm^{-1} . The bands at 1724 , 1374 and 1238 cm^{-1} were associated to acetyl acids connected to the structure of oligomers and they were ascribed to the C=O stretching, to the symmetric CH_3 bending and to the C-O stretching vibration of acetyl groups, respectively (Dávila et al., 2021).

The small peak observed at 1517 cm^{-1} can be due to the C=C stretching of aromatic rings, which may indicate the presence of a small fraction of lignin associated with the hemicellulose structure (Dávila et al., 2016; Rico et al., 2018).

The wide band around 3357 cm^{-1} was assigned to the stretching vibrations of O-H bonds of aromatic and aliphatic groups, while the band observed between 2850 and 3000 cm^{-1} could correspond to the C-H stretching (Dávila et al., 2021; Gullón et al., 2018a).

Finally, the peak at 1651 cm^{-1} has been assigned to water bound to oligosaccharides (Jiang et al., 2014).

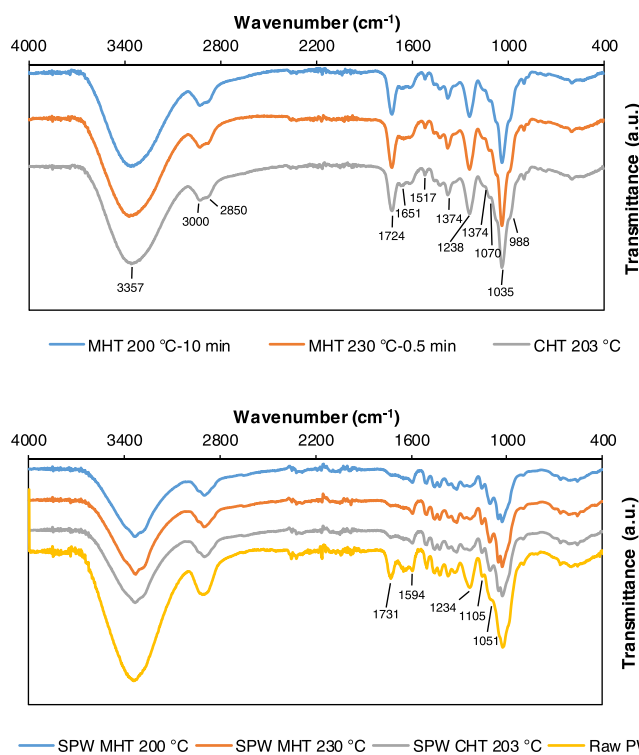


Fig. 3. FTIR spectra of the (a) liquors and (b) raw PW and pretreated PW after microwave hydrothermal treatment at 200 °C for 10 min, and 230 °C for 0.5 min, and conventional hydrothermal treatment at 203 °C .

3.3. Antioxidant profile of autohydrolysis liquors

3.3.1. Measurement of phenolic compounds and antioxidant capacity

According to the literature (Del Castillo-Llamas et al., 2021; Gullón et al., 2017a; Rico et al., 2018; Rivas et al., 2020) it has also been stated that hydrothermal processing allows the solubilization of different bioactive molecules such as phenolic compounds. In this sense, another features evaluated in this study was the antioxidant potential of the hydrothermal hydrolysates from PW obtained under conditions that led to the maximum content of soluble xylan-derivative compounds ($S_0 = 3.98$). Table 2 shows the profile of the liquors after microwave and conduction-convection heating autohydrolysis pretreatment of PW in terms of phenolic compounds and antioxidants capacity (measured with DPPH, ABTS and FRAP tests).

Regarding these data, the TPC and TFC ranged from 22.5 to 25.6 mg GAE/g PW and 27.1 – 29.4 mg RE/g PW , respectively. The liquor obtained using MHT at 230 °C for 0.5 min shows the highest TPC and TFC values, which are significantly different ($p < 0.05$) from the other two experiments. Interestingly, these values are considerably higher than those reported for autohydrolysis liquors from various feedstocks obtained under conditions that led to the maximum XO recovery such as peanut shells (TPC: 12.6 mg GAE/g peanut shell and TFC: 7.60 mg RE/g peanut shell, (Rico et al., 2018)), vine shoots (TPC: 15.3 mg GAE/g vine shoots and TFC: 8.20 mg RE/g vine shoots, (Gullón et al., 2017a)) or poplar (TPC: 10.8 mg GAE/g poplar, (Rivas et al., 2020)).

The antioxidant capacity of autohydrolysis liquors was determined using DPPH, ABTS and FRAP assays, that have been commonly applied to evaluate the antioxidant potential of complex mixtures such as those obtained from natural sources (Gullón et al., 2018b). Like for TPC and TFC, the highest value of trolox equivalents (TE) for the three assays was obtained in the experiment carried out at 230 °C for 0.5 min. The results of the DPPH, ABTS and FRAP methods carried out with this liquor were 8.18 , 27.8 and 26.5 mg TE/g PW , respectively.

Similar results were determined in liquors obtained by hydrothermal processing of different raw materials. For instance, Gullón et al. (2017a) reported DPPH, ABTS and FRAP values of 8.20 , 35.6 and 19.9 mg TE/g of vine shoots, respectively, in ethyl acetate extracts of shoot autohydrolysis liquors ($S_0 = 4.01$) and Rivas et al. (2020) reached ABTS and FRAP values of 29.7 and 18.7 mg TE/g poplar wood, respectively, while the DPPH value (1.75 mg TE/g poplar wood) was considerably lower than that found here.

3.3.2. Qualitative assessment of the polyphenolic profile of Paulownia extracts

With the intention of obtaining more information regarding the antioxidant compounds present in the liquors from CHT and MHT performed at $S_0 = 3.98$, a liquid-liquid extraction was carried out employing ethyl acetate and the extracts were analyzed by HPLC-ESI-MS. As far as the authors know, this is the first tentative identification of the profile of phenolic compounds isolated by hydrothermal

Table 2

Effect of type of heating on the TPC, TFC and antioxidant capacity of autohydrolysis liquors.

	MHT 200 °C - 10 min	MHT 230 °C - 0.5 min	CHT 203 °C
TPC (mg GAE/g raw PW)	22.5 ± 0.20^a	25.6 ± 0.46^b	22.8 ± 0.32^a
TFC (mg RE/g raw PW)	27.1 ± 0.04^a	29.4 ± 0.48^b	27.7 ± 0.13^a
DPPH (mg TE/g raw PW)	7.60 ± 0.06^a	8.18 ± 0.15^b	7.60 ± 0.05^a
ABTS (mg TE/g raw PW)	24.1 ± 0.82^b	27.8 ± 0.40^c	20.8 ± 0.48^a
FRAP (mg TE/g raw PW)	24.1 ± 0.82^a	26.5 ± 0.53^b	24.4 ± 0.57^a

processing from Paulownia wood. The compounds were identified grounded on the following criteria: (i) the measurement of the accurate mass of pseudomolecular ion [M-H]⁻ compared to the theoretical mass (with a deviation between the theoretical and the measured mass lower than 10 ppm) and (ii) the mSigma value lower than 50.

The three extracts presented the same composition, with 11 different compounds tentatively identified (see Table 3). The main phenolic acids found in this work were caffeic acid, ferulic acid, gallic acid, *p*-cumaric acid, *p*-hydroxybenzoic acid and protocatechuic acid. Regarding flavonoids, catechin, di-O-methyl quercetin B, and epigallocatechin were detected in the three extracts. In agreement with the literature, some of these compounds were formerly detected in leaves, bark and flowers of *Paulownia tomentosa* (Uğuz and Kara, 2019). Several studies have shown that these phytochemicals present multiple biological properties. For example, Semaming et al. (2014) indicated that protocatechuic acid might be helpful to prevent cardiovascular complications in diabetic patients. Ferulic acid has a protective role on cellular structures and inhibition of melanogenesis (Zduńska et al., 2018). Gallic acid has been reported as a potential therapeutic agent for managing diseases such as ulcerative colitis (Zhu et al., 2019) and rheumatoid arthritis (Fikry et al., 2019) due to its anti-inflammatory effects. Flavonoids have a wide-ranging spectrum of effects to improve health and are used in the formulation of different nutraceutical, pharmaceutical, medicinal and cosmetic products (Panche et al., 2016). In particular, catechins possess antibacterial, anti-hypertensive, anti-obesity, anti-inflammatory, anti-diabetic, and anti-carcinogenic activities (Chen et al., 2016).

3.4. Effect of microwave hydrothermal treatment and conventional hydrothermal treatment on the composition of the spent solids

Table 4 displays the data of substrate solubilization and the chemical composition of the solid fraction obtained after MHT at 200 and 230 °C at different reaction times, which correspond to severity values of the treatment in the range of 2.91–4.66.

As expected, the solubilization of the feedstock raised continuously with the severity of the treatment, from 12.7 g/100 g of raw PW at the lowest severity conditions and achieving a maximum value of 34.6 g/100 g of raw PW at the highest severity. The values of solubilization are closely related to the type of biomass used and with the severity of the treatment. Within this background, the percentages of substrate solubilization in the most severe operational conditions were close to those reported for *Populus euramericana* (31.8% at $S_0 = 4.22$) (Rivas et al., 2020), and substantially lower than those determined for chestnut shells (42.5% at $S_0 = 4.23$) (Gullón et al., 2018a) and for corn residues (49.8–52.0% at $S_0 = 4.66$) (Aguilar-Reynosa et al., 2017).

The resulting solids after MHT were mainly composed of glucan and lignin, that reflect a lesser susceptibility to hydrothermal processing, and became more enriched in these two fractions with the severity of the

Table 3
Tentative identification of phytochemicals in PW extracts.

Compound	Class/ Subclass*	Molecular Formula	<i>m/z</i> meas.	mSigma
Caffeic acid	PA/HC	C ₉ H ₈ O ₄	179.0348	9.2
Caffeic acid glucoside	PA/HC	C ₁₅ H ₁₈ O ₉	341.0909	13
Ferulic acid	PA/HC	C ₁₀ H ₁₀ O ₄	193.0497	8.6
Gallic acid	PA/HB	C ₇ H ₆ O ₅	169.0139	3.3
<i>p</i> -cumaric acid	PA/HC	C ₉ H ₈ O ₃	163.0398	14.6
<i>p</i> -hydroxybenzoic acid	PA/HB	C ₇ H ₆ O ₃	137.0242	7.2
Protocatechuic acid	PA/HB	C ₇ H ₆ O ₄	153.0193	2.4
Protocatechuic acid methyl ester	PA/HB	C ₈ H ₈ O ₄	167.0342	5.8
Di-O-methylquercetin B	FL/Flavonol	C ₁₇ H ₁₄ O ₇	329.0666	19
Epigallocatechin	FL/flavanol	C ₁₅ H ₁₄ O ₇	305.0664	17.1
Catechin	FL/Flavanol	C ₁₅ H ₁₄ O ₆	289.0714	4.4

*Abbreviations: PA: phenolic acid; HB: hydroxybenzoic acid; HC: hydroxycinnamic acid; FL: flavanoids.

Table 4

Characterization of the solid phase of PW after MHT at 200 and 230 °C, regarding solubilization and polymeric content.

MHT 200 °C					
Time (min)	Severity, S_0	Solubilization (g/100 g raw PW)	Glucan (g/100 g pretreated PW)	Hemicelluloses	Lignin
0	2.92	12.7	46.0 ± 0.46	17.9 ± 0.14	25.9 ± 0.39
5	3.72	25.0	54.3 ± 0.86	9.52 ± 0.65	28.5 ± 0.16
8	3.90	26.0	54.6 ± 1.05	8.57 ± 0.35	30.0 ± 0.79
10	3.98	27.4	55.5 ± 0.24	7.52 ± 0.17	31.1 ± 0.53
12	4.06	29.9	56.2 ± 0.27	6.40 ± 0.10	31.6 ± 0.13
15	4.15	31.1	57.3 ± 0.18	5.77 ± 0.09	32.8 ± 0.76
20	4.26	32.0	57.6 ± 0.01	5.27 ± 0.05	33.4 ± 0.79
24	4.34	31.4	57.9 ± 1.17	5.03 ± 0.11	33.1 ± 0.01
32	4.46	31.6	58.4 ± 0.29	3.54 ± 0.03	34.0 ± 0.16
50	4.65	33.1	58.2 ± 0.63	3.19 ± 0.09	35.9 ± 0.46
MHT 230 °C					
Time (min)	Severity, S_0	Solubilization (g/100 g raw PW)	Glucan (g/100 g pretreated PW)	Hemicelluloses	Lignin
0	3.77	28.2	56.2 ± 0.19	9.01 ± 0.73	29.8 ± 0.49
0.25	3.88	29.0	56.4 ± 0.78	7.06 ± 0.01	30.3 ± 0.31
0.5	3.98	28.8	57.3 ± 0.33	6.36 ± 0.05	30.4 ± 0.31
0.75	4.04	29.5	58.0 ± 0.89	5.49 ± 0.65	30.6 ± 0.34
1	4.10	31.7	58.4 ± 0.04	4.78 ± 0.05	31.2 ± 0.53
1.25	4.15	31.8	59.0 ± 0.08	4.15 ± 0.14	31.1 ± 0.26
1.42	4.19	32.6	59.3 ± 0.26	3.95 ± 0.00	31.8 ± 1.02
2	4.29	32.6	59.7 ± 0.01	3.30 ± 0.18	34.6 ± 0.56
3	4.42	33.3	59.8 ± 0.48	2.84 ± 0.13	35.2 ± 0.32
6	4.66	34.6	60.4 ± 0.68	1.88 ± 0.05	32.8 ± 0.50

treatment. The glucan was the major component, and its content augmented remarkably from 46.0 to 58.2 g/100 g pretreated PW when the experiments were performed from 0 to 50 min at 200 °C, while a less marked increase was observed in treatments performed at 230 °C between 0 and 6 min (56.2–60.4 g/100 g pretreated PW). These values represented an average of 95% of the initial glucan contained in the raw material.

The content of Klason lignin increased steadily with the time reaction, being the highest value reached 35.9 g/100 g pretreated PW for the most severe condition ($S_0 = 4.66$, corresponding to 200 °C and 50 min).

Oppositely to the behavior of the glucan and lignin fractions, the content of hemicelluloses (xylan, arabinan and acetyl groups) in spent solids decreased progressively with the severity, owing to the susceptibility of this fraction to hydrolysis reactions. As it can be seen in the data listed in Table 4, the time required to achieve an almost complete removal of this fraction was less for the highest temperature studied (94% in the experiment performed during 6 min at 230 °C versus 90% in the one carried out for 50 min at 200 °C). Our results were also in line

with those obtained by Rivas et al. (2020), who reported a complete solubilization of hemicelluloses from *Populus euramericana* operating a $S_0 = 4.53$. Overall, the positive impact of the temperature and residence time on the hydrolysis of the hemicelluloses was formerly reported by Remón et al. (2018) and Dávila et al. (2021).

It should be noted that the harshest conditions studied ($S_0 = 4.66$) resulted in a solid mainly composed by glucan (60.4 g/100 g pretreated PW) and lignin (32.8 g/100 g pretreated PW) in the treatment carried out at 230 °C for 6 min. In addition, del Río et al. (2020a) also reported a spent solid mostly constituted by glucan and lignin (54.21% and 41.20%) when PW was treated at $S_0 = 4.68$, corresponding to non-isothermal CHT at 230 °C.

Hence, some authors have been suggested a subsequent fractionation of this exhausted solid to recover glucan and lignin separately in order to achieve an integral valorization of the lignocellulosic materials following a multiproduct biorefinery approach (Del Castillo-Llamosas et al., 2021; Rico et al., 2018).

In addition to evaluating the impact of the heating system on the

chemical characterization of the autohydrolysis hydrolysates, its influence on the composition of the spent obtained solids was also studied under the conditions that led to a maximum concentration of XO. Briefly, the heating system did not noticeably affect the composition of these solids. On the one hand, the lignin and hemicelluloses content was slightly lower employing conventional-heating autohydrolysis than that obtained by MHT (29.8% and 5.85% vs 30.75% and 6.94%, respectively). Regarding the glucan fraction, its content was barely higher in the solid obtained by autohydrolysis via conventional heating (58.1% vs 56.4%), due to increased removal of hemicelluloses (81% vs 77%).

3.5. Structural characterization of the spent solids after autohydrolysis

In order to evaluate the impact that the type of heating could exert on the morphology and structure of autohydrolyzed solids, and how these modifications (removal of hemicelluloses and relocation of lignin) may affect its use for biofuel production (via enzymatic-fermentative pathway), FTIR and SEM assays were performed.

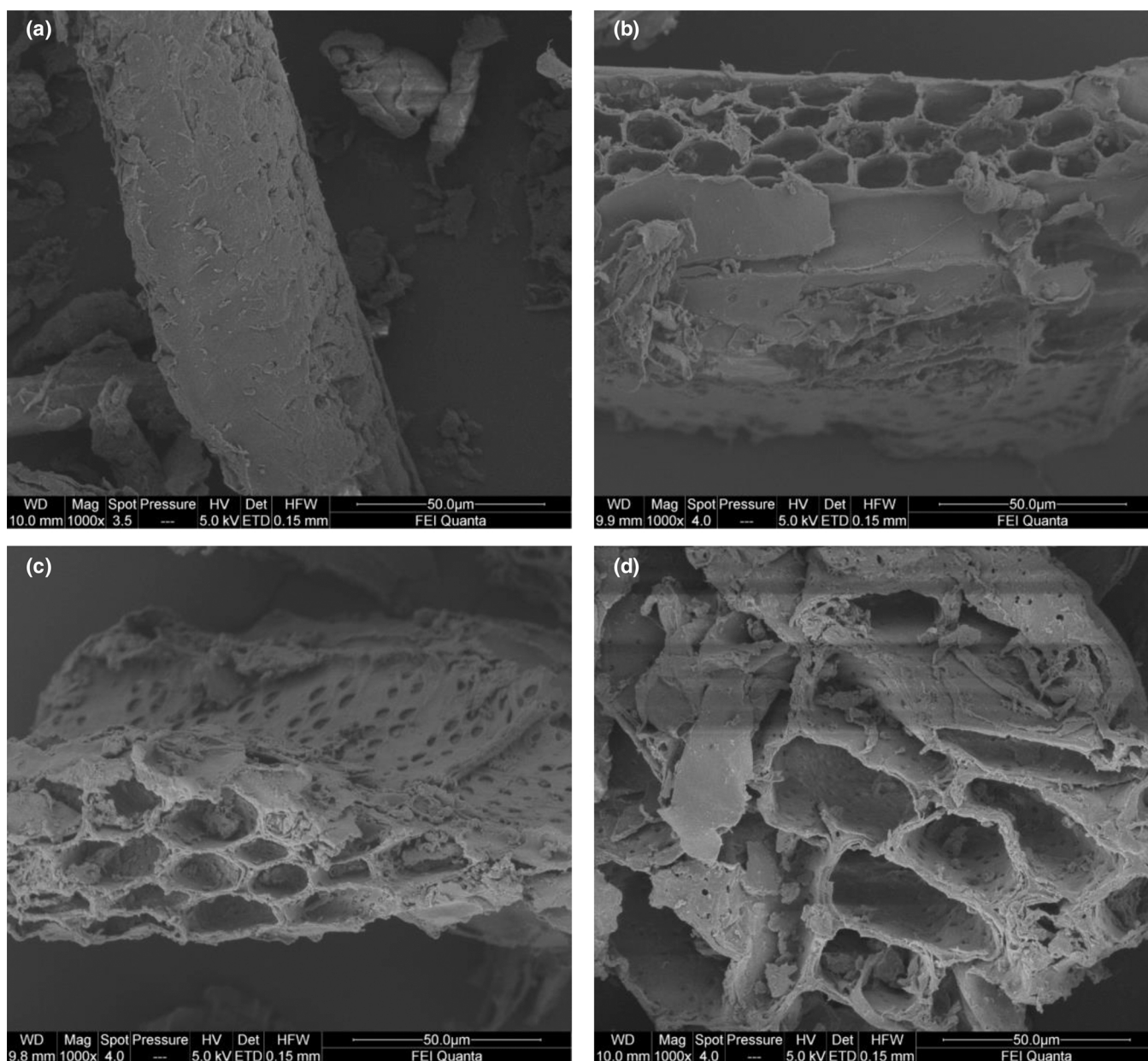


Fig. 4. SEM of: (a) raw PW, (b) PW after MHT at 200 °C for 10 min, (c) MHT at 230 °C for 0.5 min, and (d) CHT at 203 °C.

Fig. 3b shows the FTIR spectra of the untreated Paulownia, the spent solids obtained in CHT and in MHT performed at $S_0 = 3.98$. As can be seen, the FTIR spectra of the three solids recovered from hydrothermal processing did not present differences, however, these solids showed some differences compared to the FTIR of the starting Paulownia, mainly due to the solubilization of the hemicellulosic fraction that occurs during treatment. The removal of this fraction in the autohydrolyzed solids was evidenced in the almost complete disappearance of the peak at 1731 cm^{-1} which is associated with the stretching vibration of the C=O groups of the acetyl ester units of the hemicelluloses (Dávila et al., 2021; Guleria et al., 2018). This removal can also be associated with the C-O stretching of acetyl groups from hemicelluloses, resulting in a reduction in the intensity of the signal at 1234 cm^{-1} (Dávila et al., 2021).

Compared with the starting Paulownia, in the FTIR spectra of the spent solids from CHT and MHT it was possible to observe two new bands at 1105 and 1053 cm^{-1} ascribed to the structure of the cellulose (Dávila et al., 2021; Galia et al., 2015). Furthermore, the intensity of peak at 1594 cm^{-1} which is associated with the vibrations of lignin aromatic of lignin was more intense in the spent solids (Dávila et al., 2021; Galia et al., 2015).

Fig. 4 displays the SEM micrographs of raw PW and PW after MHT and CHT at $S_0 = 3.98$. The use of autohydrolysis, either assisted by microwaves or by conventional heating, provoked the disruption of PW. In this context, the surface structure of PW seemed flat, packed, firm and smooth, while pretreated PW exhibited unsmooth, uneven and wrecked surface (Thakur et al., 2012), that may enhance their enzymatic digestibility, improving the contact of enzyme and PW. Similar behaviors were observed for birch wood after steam explosion (Kalyani et al., 2017), or vine shoots subjected to CHT (Jesus et al., 2017).

3.6. Enzymatic hydrolysis of autohydrolyzed spent solids

With the final aim of evaluating the digestibility of the resulting spent solids after autohydrolysis (via microwave or conventional heating), enzymatic hydrolysis was performed at favorable conditions

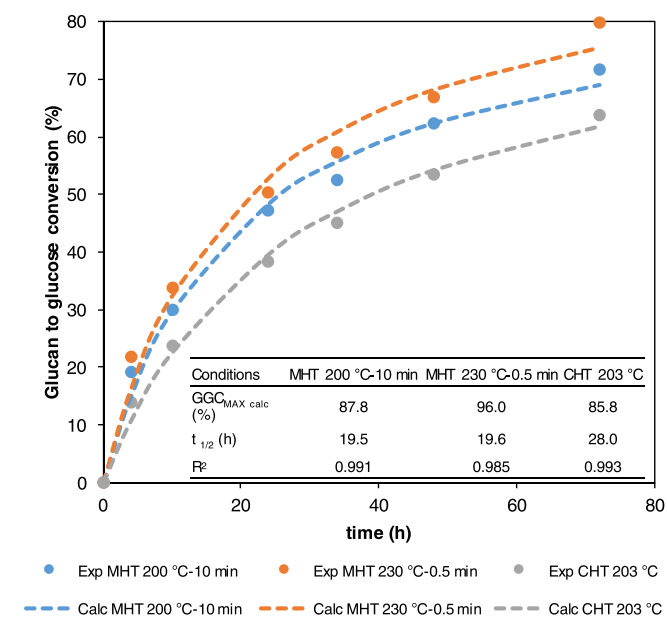


Fig. 5. Glucan to glucose conversion (GGC), calculated maximum glucan to glucose conversion ($GGC_{MAX\text{ calc}}$), $t_{1/2}$ and R^2 obtained from the enzymatic susceptibility of autohydrolyzed PW using microwave-heating at 200 °C for 10 min, 230 °C for 0.5 min, and conventional-heating at 203 °C . Dots represent the experimental value of GGC (Exp) and dotted lines the calculated value from Holtzapple equation (Calc).

($C=5\text{ g}/100\text{ g}$, $CSR=20\text{ FPU}/\text{g}$). Fig. 5 exhibits the results from Holtzapple modelization as well as the time course of experimental and calculated glucan to glucose conversion (GGC) during 72 h. In this sense, fast GGC are obtained within the first 24 h, reaching between 39.6% and 52.8%. It is already noteworthy at this time, that PW after microwave heating behaves as a more susceptible biomass than that obtained from CHT. At 72 h, the final GGC achieved was 63.8% for CHT, 71.8% for MHT at 200 °C for 10 min, and 79.7% for MHT at 230 °C for 0.5 min, reflecting the effectiveness of microwave to obtain solids with higher enzymatic susceptibility.

These data may be compared with the literature, for example del Río et al. (2020b) reached up to a glucan to glucose conversion of 65.5% at 72 h with autohydrolyzed corn stover at 200 °C ($S_0 = 3.93$), which corresponds with the maximum of xylooligosaccharides. In another study, Romani et al. (2010) obtained only a 40% of cellulose to glucose conversion at 72 h from *Eucalyptus globulus* autohydrolyzed at the condition conducting to maximum recovery of oligosaccharides (195 °C , $S_0 = 3.64$).

On the other hand, the Holtzapple equation aid an efficient fitting of the experimental data with R^2 between 0.985 and 0.993, determining a $GGC_{MAX\text{ calc}}$ at infinite time of between 85.8% and 96.0%. Another concept to bear in mind is the time needed to obtain half of the GGC, which reflect the speed of the hydrolysis reaction. In this sense, values of $t_{1/2}$ of 19.5–19.6 h were obtained when employing microwave heating, while after conventional heating, the $t_{1/2}$ increased to 28.0 h which implied 1.4-fold higher time.

3.7. Energy consumption analysis for the two heating mechanisms

In addition to the previous information reported for the solid and liquid fractions obtained from MHT and CHT, the energy consumed during the processing is also a crucial point to bear in mind since the pretreatment represents about the 20% of the total cost within a biorefinery for biofuel production (Yang and Wyman, 2007).

In this sense, the effect of the heating mechanism leading to the conditions that permitted maximizing the production of XO ($S_0 = 3.98$) were performed both in MHT and CHT. Fig. 6 shows the temperature profiles to achieve the same treatment severity using both heating systems. As can be appreciate, the time required to achieve the target temperature (and maintain it in the isothermal treatments) was notably longer in conventionally heated autohydrolysis than in microwave-assisted treatment: 35 min vs 15 and 5.5 min in MHT at 200 °C for 10 min and 230 °C for 0.5 min, respectively. Regarding the cooling stage, in the MHT were needed about 4.5 min to reach 85 °C , while in the CHT Büchiglasuster reactor 16 min were required to achieve that temperature.

Consequently, the energy consumed was determined regarding the power employed and the PW processed, and the results were: 24.5 MJ/

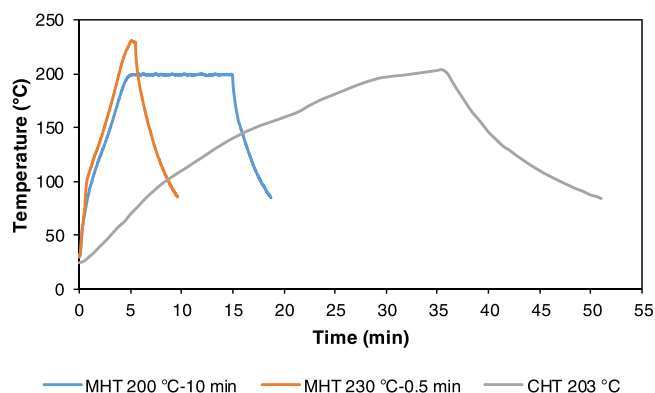


Fig. 6. Time course of the temperature profiles for MHT at 200 °C for 10 min, 230 °C for 0.5 min and CHT at 203 °C .

kg for MHT 200 °C for 10 min, 18.3 MJ/kg for MHT 230 °C for 0.5 min, and 51.8 MJ/kg for non-isothermal CHT at 203 °C. In this sense, conventionally heated autohydrolysis accounted for 2.1 and 2.8-fold higher energy consumption in contrast to MHT at 200 and 230 °C, at the same severity of 3.98. In this sense, microwave-assisted autohydrolysis can be highlighted as a more sustainable and energy-efficient heating technology if compared to CHT.

The values obtained can be compared with those reported by Dávila et al. (2021) when estimating the energy consumption of microwave and conventionally-assisted autohydrolysis of vine shoots. In this case, 150 W·h were necessary for the microwave-assisted treatment of vine shoots at 180 °C for 20 min (condition conducting to the highest quantity of oligosaccharides), while in our study 7.76 and 5.79 W·h were needed for the experiments performed at 200 °C for 10 min and 230 °C for 0.5 min, respectively. Regarding CHT, about 520 W·h were required for the processing of vine shoots at 180 °C for 15 min, while PW pretreatment spent 860 W·h to perform non-isothermal autohydrolysis at 203 °C. In this sense, a lower amount of energy is consumed in this work during microwave processing, while higher energy consumption is performed for CHT in comparison with Dávila et al. (2021).

4. Conclusion

Microwave hydrothermal treatment is a promising technology for the valorization of Paulownia wood as first step of a biorefinery. Although slight differences were found for the chemical composition of solid and liquid fractions, and for the structural characterization of the liquors, interesting variations were observed in the solid fraction behavior to enzymes reaching higher glucan to glucose conversions if compared to conventional-heating autohydrolysis. Additionally, energy of 18.3–24.5 MJ/kg was consumed by microwave heating, in contrast to 51.8 MJ/kg for conventional heating. These data reveal that microwave hydrothermal treatment is a more efficient, eco-friendlier method for the valorization of Paulownia wood.

CRedit authorship contribution statement

Pablo G. del Río: Formal analysis, Investigation, Methodology, Writing – original draft, Visualization, Writing – review & editing. **Alba Pérez-Pérez:** Investigation, Visualization. **Gil Garrote:** Funding acquisition, Supervision, Validation, Writing – review & editing. **Beatriz Gullón:** Conceptualization, Formal analysis, Funding acquisition, Investigation, Methodology, Validation, Writing – original draft, Visualization, Writing – review & editing.

Declaration of Competing Interest

The authors declare that they have no known competing financial interests or personal relationships that could have appeared to influence the work reported in this paper.

Data Availability

Data will be made available on request.

Acknowledgments

Authors are grateful to the University of Vigo and CISUG for the financial support of Open Access publication, to MINECO (Spain) for the financial support of this work in the framework of the projects “Cutting-edge strategies for a sustainable biorefinery based on valorization of invasive species” with reference PID2019-110031RB-I00 and to Consellería de Cultura, Educación e Ordenación Universitaria (Xunta de Galicia) through the contract ED431C 2017/62-GRC to Competitive Reference Group BV1, programs partially funded by ERDF. Pablo G. del Río and Beatriz Gullón would like to express their gratitude to the

Ministry of Science, Innovation and Universities of Spain for his FPU research grant (FPU16/04077) and her RYC grant (Grant reference RYC2018-026177-I), respectively.

Appendix A. Supplementary material

Supplementary data associated with this article can be found in the online version at doi:10.1016/j.indcrop.2022.115313.

References

- Adney, B., Baker, J., 2008. Measurement of Cellulase Activities: Laboratory Analytical Procedure (LAP), Technical report: NREL/TP-510-42628, NREL (National Renewable Energy Laboratory).
- Aguilar-Reynosa, A., Romaní, A., Rodríguez-Jasso, R.M., Aguilar, C.N., Garrote, G., Ruiz, H.A., 2017. Comparison of microwave and conduction-convection heating autohydrolysis pretreatment for bioethanol production. *Bioresour. Technol.* 243, 273–283. <https://doi.org/10.1016/j.biortech.2017.06.096>.
- Álvarez, C., González, A., Negro, M.J., Ballesteros, I., Oliva, J.M., Sáez, F., 2017. Optimized use of hemicellulose within a biorefinery for processing high value-added xylooligosaccharides. *Ind. Crop. Prod.* 99, 41–48. <https://doi.org/10.1016/j.indcrop.2017.01.034>.
- Blasa, M., Candiracci, M., Accorsi, A., Piacentini, M.P., Albertini, M.C., Piatti, E., 2005. Raw *Millefiori* honey is packed full of antioxidants. *Food Chem.* 97, 217–222. <https://doi.org/10.1016/j.foodchem.2005.03.039>.
- Blumenkrantz, N., Asboe-Hansen, G., 1973. New method for quantitative determination of uranic acids. *Anal. Biochem.* 54, 484–489. [https://doi.org/10.1016/0003-2697\(73\)90377-1](https://doi.org/10.1016/0003-2697(73)90377-1).
- Chen, X.Q., Hu, T., Han, Y., Huang, W., Yuan, H.B., Zhang, Y.T., Du, Y., Jiang, Y.W., 2016. Preventive effects of catechins on cardiovascular disease. *Molecules* 21, 1–7. <https://doi.org/10.3390/molecules21121759>.
- Dávila, I., Gordobil, O., Labidi, J., Gullón, P., 2016. Assessment of suitability of vine shoots for hemicellulosic oligosaccharides production through aqueous processing. *Bioresour. Technol.* 211, 636–644. <https://doi.org/10.1016/j.biortech.2016.03.153>.
- Dávila, I., Gullón, B., Alonso, J.L., Labidi, J., Gullón, P., 2019. Vine shoots as new source for the manufacture of prebiotic oligosaccharides. *Carbohydr. Polym.* 207, 34–43. <https://doi.org/10.1016/j.carbpol.2018.11.065>.
- Dávila, I., Gullón, P., Labidi, J., 2021. Influence of the heating mechanism during the aqueous processing of vine shoots for the obtaining of hemicellulosic oligosaccharides. *Waste Manag.* 120, 146–155. <https://doi.org/10.1016/j.wasman.2020.11.014>.
- Del Castillo-Llamas, A., Rodríguez-Martínez, B., del Río, P.G., Eibes, G., Garrote, G., Gullón, B., 2021. Hydrothermal treatment of avocado peel waste for the simultaneous recovery of oligosaccharides and antioxidant phenolics. *Bioresour. Technol.* 342, 125981. <https://doi.org/10.1016/j.biortech.2021.125981>.
- del Río, P.G., Domínguez, V.D., Domínguez, E., Gullón, P., Gullón, B., Garrote, G., Romaní, A., 2020a. Comparative study of biorefinery processes for the valorization of fast-growing Paulownia wood. *Bioresour. Technol.* 314, 123722. <https://doi.org/10.1016/j.biortech.2020.123722>.
- del Río, P.G., Gullón, P., Rebelo, F.R., Romaní, A., Garrote, G., Gullón, B., 2020b. A whole-slurry fermentation approach to high-solid loading for bioethanol production from corn stover. *Agronomy* 10, 1790. <https://doi.org/10.3390/agronomy10111790>.
- del Río, P.G., Gullón, B., Romaní, A., Garrote, G., 2021. Fast-growing Paulownia wood fractionation by microwave-assisted hydrothermal treatment: a kinetic assessment. *Bioresour. Technol.* 338, 125535. <https://doi.org/10.1016/j.biortech.2021.125535>.
- Domínguez, E., Nóvoa, T., del Río, P.G., Garrote, G., Romaní, A., 2020. Sequential two-stage autohydrolysis biorefinery for the production of bioethanol from fast-growing Paulownia biomass. *Energy Convers. Manag.* 226, 113517. <https://doi.org/10.1016/j.enconman.2020.113517>.
- Dżugan, M., Miłek, M., Grabek-Lejko, D., Hęćlik, J., Jacek, B., Litwińczuk, W., 2021. Antioxidant activity, polyphenolic profiles and antibacterial properties of leaf extract of various *Paulownia* spp. Clones. *Agronomy* 11. <https://doi.org/10.3390/agronomy11102001>.
- Fikry, E.M., Gad, A.M., Eid, A.H., Arab, H.H., 2019. Caffeic acid and ellagic acid ameliorate adjuvant-induced arthritis in rats via targeting inflammatory signals, chitinase-3-like protein-1 and angiogenesis. *Biomed. Pharmacother.* 110, 878–886. <https://doi.org/10.1016/j.biopha.2018.12.041>.
- Galia, A., Schiavo, B., Antonetti, C., Galletti, A.M.R., Interrante, L., Lessi, M., Scialdone, O., Valenti, M.G., 2015. Autohydrolysis pretreatment of *Arundo donax*: a comparison between microwave-assisted batch and fast heating rate flow-through reaction systems. *Biotechnol. Biofuels* 8, 1–18. <https://doi.org/10.1186/s13068-015-0398-5>.
- González-García, S., Morales, P.C., Gullón, B., 2018. Estimating the environmental impacts of a brewery waste-based biorefinery: bio-ethanol and xylooligosaccharides joint production case study. *Ind. Crop. Prod.* 123, 331–340. <https://doi.org/10.1016/j.indcrop.2018.07.003>.
- Guleria, A., Singha, A.S., Rana, R.K., 2018. Mechanical, thermal, morphological, and biodegradable studies of okra cellulose fiber reinforced starch-based biocomposites. *Adv. Polym. Technol.* 37, 104–112. <https://doi.org/10.1002/adv.21646>.
- Gullón, B., Gullón, P., Tavaría, F., Pintado, M., Gomes, A.M., Alonso, J.L., Parajó, J.C., 2014. Structural features and assessment of prebiotic activity of refined

- arabinoxyloligosaccharides from wheat bran. *J. Funct. Foods* 6, 438–449. <https://doi.org/10.1016/j.jff.2013.11.010>.
- Gullón, B., Eibes, G., Moreira, M.T., Dávila, I., Labidi, J., Gullón, P., 2017a. Antioxidant and antimicrobial activities of extracts obtained from the refining of autohydrolysis liquors of vine shoots. *Ind. Crop. Prod.* 107, 105–113. <https://doi.org/10.1016/j.indcrop.2017.05.034>.
- Gullón, B., Gullón, P., Lú-Chau, T.A., Moreira, M.T., Lema, J.M., Eibes, G., 2017b. Optimization of solvent extraction of antioxidants from *Eucalyptus globulus* leaves by response surface methodology: characterization and assessment of their bioactive properties. *Ind. Crop. Prod.* 108, 649–659. <https://doi.org/10.1016/j.indcrop.2017.07.014>.
- Gullón, B., Eibes, G., Dávila, I., Moreira, M.T., Labidi, J., Gullón, P., 2018a. Hydrothermal treatment of chestnut shells (*Castanea sativa*) to produce oligosaccharides and antioxidant compounds. *Carbohydr. Polym.* 192, 75–83. <https://doi.org/10.1016/j.carbpol.2018.03.051>.
- Gullón, B., Gullón, P., Eibes, G., Cara, C., De Torres, A., López-Linares, J.C., Ruiz, E., Castro, E., 2018b. Valorisation of olive agro-industrial by-products as a source of bioactive compounds. *Sci. Total Environ.* 645, 533–542. <https://doi.org/10.1016/j.scitotenv.2018.07.155>.
- Holtzapfel, M.T., Caram, H.S., Humphrey, A.E., 1984. A comparison of two empirical models for the enzymatic hydrolysis of pretreated poplar wood. *Biotechnol. Bioeng.* 26, 936–941. <https://doi.org/10.1002/bit.260260818>.
- Jeong, S.Y., Lee, J.W., 2015. Hydrothermal treatment. *Pretreatment of Biomass: Processes and Technologies*, pp. 61–74. (<https://doi.org/10.1016/B978-0-12-800080-9.00005-0>).
- Jesus, M.S., Román, A., Genisheva, Z., Teixeira, J.A., Domingues, L., 2017. Integral valorization of vine pruning residue by sequential autohydrolysis stages. *J. Clean. Prod.* 168, 74–86. <https://doi.org/10.1016/j.jclepro.2017.08.230>.
- Jiang, H., Chen, Q., Ge, J., Zhang, Y., 2014. Efficient extraction and characterization of polymeric hemicelluloses from hybrid poplar. *Carbohydr. Polym.* 101, 1005–1012. <https://doi.org/10.1016/j.carbpol.2013.10.030>.
- Jönsson, L.J., Martín, C., 2016. Pretreatment of lignocellulose: formation of inhibitory by-products and strategies for minimizing their effects. *Bioresour. Technol.* 199, 103–112. <https://doi.org/10.1016/j.biortech.2015.10.009>.
- Kalyani, D.C., Zamanzadeh, M., Müller, G., Horn, S.J., 2017. Biofuel production from birch wood by combining high solid loading simultaneous saccharification and fermentation and anaerobic digestion. *Appl. Energy* 193, 210–219. <https://doi.org/10.1016/j.apenergy.2017.02.042>.
- Li, W., Cao, J., Yang, J., Wang, Z., Yang, Y., 2021. Production and characterization of lignocellulosic fractions from sisal waste. *Ind. Crop. Prod.* 160, 113109. <https://doi.org/10.1016/j.indcrop.2020.113109>.
- López-Linares, J.C., García-Cubero, M.T., Lucas, S., González-Benito, G., Coca, M., 2019. Microwave assisted hydrothermal as greener pretreatment of brewer's spent grains for biobutanol production. *Chem. Eng. J.* 368, 1045–1055. <https://doi.org/10.1016/j.cej.2019.03.032>.
- Panche, A.N., Diwan, A.D., Chandra, S.R., 2016. Flavonoids: an overview. *J. Nutr. Sci.* 5, 1–15. <https://doi.org/10.1017/jns.2016.41>.
- Remón, J., Santomauro, F., Chuck, C.J., Matharu, A.S., Clark, J.H., 2018. Production of fermentable species by microwave-assisted hydrothermal treatment of biomass carbohydrates: reactivity and fermentability assessments. *Green Chem.* 20, 4507–4520. <https://doi.org/10.1039/c8gc02182a>.
- Rico, X., Gullón, B., Alonso, J.L., Parajó, J.C., Yáñez, R., 2018. Valorization of peanut shells: manufacture of bioactive oligosaccharides. *Carbohydr. Polym.* 183, 21–28. <https://doi.org/10.1016/j.carbpol.2017.11.009>.
- Rivas, S., Rigual, V., Domínguez, J.C., Alonso, M.V., Olliet, M., Parajó, J.C., Rodríguez, F., 2020. A biorefinery strategy for the manufacture and characterization of oligosaccharides and antioxidants from poplar hemicelluloses. *Food Bioprod. Process.* 123, 398–408. <https://doi.org/10.1016/j.fbp.2020.07.018>.
- Romaní, A., Garrote, G., Alonso, J.L., Parajó, J.C., 2010. Bioethanol production from hydrothermally pretreated *Eucalyptus globulus* wood. *Bioresour. Technol.* 101, 8706–8712. <https://doi.org/10.1016/j.biortech.2010.06.093>.
- Semaming, Y., Kumfu, S., Pannangpetch, P., Chattipakorn, S.C., Chattipakorn, N., 2014. Protocatechuic acid exerts a cardioprotective effect in type 1 diabetic rats. *J. Endocrinol.* 223, 13–23. <https://doi.org/10.1530/JOE-14-0273>.
- Singleton, V.L., Rossi, J.A.J., 1965. Colorimetry to total phenolics with phosphomolybdic acid reagents. *Am. J. Enol. Vinic.* 16, 144–158.
- Sluiter, A., Hames, B., Hyman, D., Payne, C., Ruiz, R., Scarlata, C., Sluiter, J., Templeton, D., Wolfe, J., 2008a. Determination of Total Solids in Biomass and Total Dissolved Solids in Liquid Process Samples. *Laboratory Analytical Procedure (LAP)*. National Renewable Energy Laboratory.
- Sluiter, A., Hames, B., Ruiz, R., Scarlata, C., Sluiter, J., Templeton, D., 2008b. Determination of Ash in Biomass. *Laboratory Analytical Procedure (LAP)*. National Renewable Energy Laboratory.
- Sluiter, A., Hames, B., Ruiz, R., Scarlata, C., Sluiter, J., Templeton, D., Crocker, D., 2008c. Determination of Structural Carbohydrates and Lignin in Biomass. *Laboratory Analytical Procedure (LAP)*. National Renewable Energy Laboratory. <https://doi.org/10.1016/j.rmr.2016.02.006>.
- Sluiter, A., Ruiz, R., Scarlata, C., Sluiter, J., Templeton, D., 2008d. Determination of Extractives in Biomass. *Laboratory Analytical Procedure (LAP)*. National Renewable Energy Laboratory. <https://doi.org/10.1016/j.rmr.2016.02.006>.
- Sluiter, J.B., Ruiz, R.O., Scarlata, C.J., Sluiter, A.D., Templeton, D.W., 2010. Compositional analysis of lignocellulosic feedstocks. 1. Review and description of methods. *J. Agric. Food Chem.* 58, 9043–9053. <https://doi.org/10.1021/jf1008023>.
- Solarte-Toro, J.C., Cardona-Alzate, C.A., 2021. Biorefineries as the base for accomplishing the sustainable development goals (SDGs) and the transition to bioeconomy: technical aspects, challenges and perspectives. *Bioresour. Technol.* 340, 125626. <https://doi.org/10.1016/j.biortech.2021.125626>.
- Solarte-Toro, J.C., Chacón-Pérez, Y., Cardona-Alzate, C.A., 2018. Evaluation of biogas and syngas as energy vectors for heat and power generation using lignocellulosic biomass as raw material. *Electron. J. Biotechnol.* 33, 52–62. <https://doi.org/10.1016/j.ejbt.2018.03.005>.
- Thakur, V.K., Singha, A.S., Thakur, M.K., 2012. Surface modification of natural polymers to impart low water absorbency. *Int. J. Polym. Anal. Charact.* 17, 133–143. <https://doi.org/10.1080/1023666X.2012.640455>.
- Uğuz, Ö., Kara, Y., 2019. Determination of antioxidant potential in the leaf and flower of *Paulownia tomentosa*. *Int. J. Second. Metab.* 6, 106–112. <https://doi.org/10.21448/ijsm.537166>.
- Yang, B., Wyman, C.E., 2007. Pretreatment: the key to unlocking low-cost cellulose ethanol. *Biofuels Bioprod. Bioref.* 2, 26–40. <https://doi.org/10.1002/bbb.49>.
- Zduńska, K., Dana, A., Kolodziejczak, A., Rotsztein, H., 2018. Antioxidant properties of ferulic acid and its possible application. *Skin Pharmacol. Physiol.* 31, 332–336. <https://doi.org/10.1159/000491755>.
- Zhu, L., Gu, P.Q., Shen, H., 2019. Gallic acid improved inflammation via NF-κB pathway in TNBS-induced ulcerative colitis. *Int. Immunopharmacol.* 67, 129–137. <https://doi.org/10.1016/j.intimp.2018.11.049>.